analytical chemistry

Article

pubs.acs.org/ac

High Speed Size Sorting of Subcellular Organelles by Flow Field-Flow Fractionation

Joon Seon Yang, Ju Yong Lee, and Myeong Hee Moon*

Department of Chemistry, Yonsei University, Seoul, 120-749 South Korea

Supporting Information

ABSTRACT: Separation/isolation of subcellular species, such as mitochondria, lysosomes, peroxisomes, Golgi apparatus, and others, from cells is important for gaining an understanding of the cellular functions performed by specific organelles. This study introduces a high speed, semipreparative scale, biocompatible size sorting method for the isolation of subcellular organelle species from homogenate mixtures of HEK 293T cells using flow field-flow fractionation (FlFFF). Separation of organelles was achieved using asymmetrical FlFFF (AF4) channel system at the steric/hyperlayer mode in which nuclei, lysosomes, mitochondria, and peroxisomes were separated in a decreasing order of hydrodynamic diameter without complicated preprocessing steps. Fractions in which organelles were not clearly separated were reinjected to AF4 for a finer separation using the normal mode, in which smaller sized species can be well fractionated by an increasing order of diameter. The subcellular species contained in collected AF4 fractions were examined with scanning electron microscopy to evaluate their size and morphology, Western blot analysis using organelle specific markers was used for organelle confirmation, and proteomic analysis was performed with nanoflow liquid chromatography-tandem mass spectrometry (nLC-ESI-MS/MS). Since FlFFF operates with biocompatible buffer solutions, it offers great flexibility in handling subcellular components without relying on a high concentration sucrose solution for centrifugation or affinity- or fluorescence tag-based sorting methods. Consequently, the current study provides an alternative, competitive method for the isolation/purification of subcellular organelle species in their intact states.

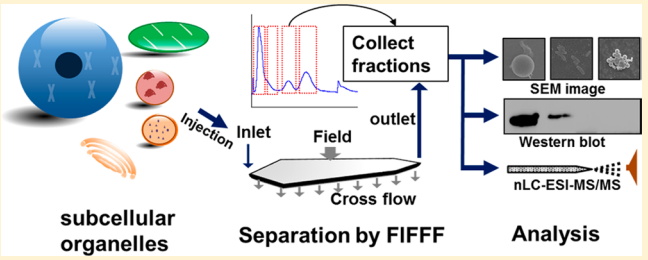

Organelles are subcellular, membrane-bounded structures found in eukaryotic cells and include the nucleus, Golgi complex, mitochondrion, endoplasmic reticulum (ER), lysosome, peroxisome, ribosome, proteasome, and others.[1−3] Since organelles have their own distinct functions, abnormalities of these organelles may influence the development of diseases directly or indirectly. For instance, it is reported that somatic mitochondrial DNA mutation caused by oxidative damage may cause neurodegenerative disorders such as Alzheimer's disease and Parkinson's disease.[4−6] A number of diseases are known to be related with different organelles: typical lysosomal storage disorders (LSD),[7] such as Gaucher and Fabry diseases, peroxisome biogenesis disorders (PBD),[8] such as Zellweger syndrome and neonatal adrenoleukodystrophy, and ER stress,[9] such as obesity, insulin resistance, and type 2 diabetes. While advances in proteomic analyses offer the capability to unveil the functions of some of the regulatory proteins, these proteins are often expressed in specific subcellular locations and are very low in abundance.[3] Therefore, selective isolation or purification of organelles is an important challenge for the development of both biomarkers and therapeutic methods.

Isolation of organelles is traditionally achieved with centrifugation methods, such as differential centrifugation and density gradient centrifugation. While centrifugation-based methods are simple to perform, they are rather time-consuming and it is difficult to achieve a pure fraction when the organelles of interests have similar densities.[2,10−12] Affinity purification utilizes an antibody which has a specific binding affinity to a protein on the surface of the organelle, yielding a relatively pure fraction of the specific organelle. However, this method relies strictly on the binding specificity of the antibody to the organelle and, moreover, available antibodies can be limiting.[2,13,14] Fluorescence-activated organelle sorting (FAOS) utilizes flow cytometry to selectively sort organelles labeled with specific fluorescent chemicals. In the literature, it has been reported for the enrichment of endosomes,[15] mitochondria,[16] and secretory granules.[17] While FAOS offers a relatively fast (<1 h) sorting of organelles with lower levels of contamination by other organelles compared to density gradient centrifugation, it requires the expression of organelle-specific fluorescent proteins and the sizes of the organelles that can be sorted are limited.

Flow field-flow fractionation (FlFFF) is an elution-based separation method that is capable of size-sorting particles and biological macromolecules like proteins, DNA, cells, and so on, without relying on a partition or an interaction of sample components with the packing materials.[18−20] Separation in

Received: March 31, 2015
Accepted: May 25, 2015
Published: May 25, 2015

DOI: 10.1021/acs.analchem.5b01207
Anal. Chem. 2015, 87, 6342−6348

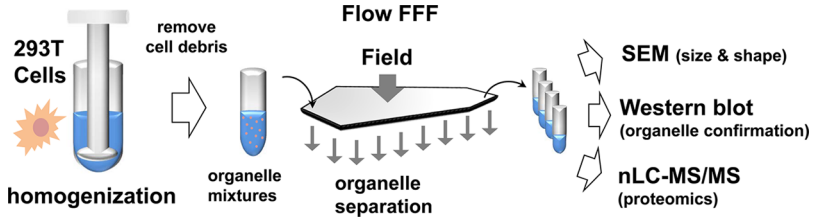

Figure 1. Scheme for organelle sorting by FlFFF and the process for confirming the presence of organelles in the collected fractions.

FlFFF is carried out in an empty, thin rectangular channel space using two different flow streams: a migration flow carrying the sample components along the channel axis to the detector and a crossflow moving across the channel cross-section to drive the sample components in the vicinity of one wall of the channel. Particles with smaller diameters diffuse faster, protrude farther against the channel wall in a direction opposite to the crossflow, and migrate down the channel faster than larger particles since the flow velocity in the parabolic flow profile increases as it moves away from the channel wall. Therefore, smaller particles elute earlier than do larger ones, according to the normal mode of FlFFF separation.[18] However, for particles larger than ~1 μm, the particles' diffusion becomes negligible and the particles migrate at or above a certain distance from the channel wall. In this case, the center of gravity (cg) of the particles determines the relative height of the particles against the wall and, thus, the migration speed, resulting in an elution of large particles first described as the steric/hyperlayer mode of separation.[21] Since separation in FlFFF takes place in an unobstructed channel with biological buffer solutions, a gentle but high speed separation of biological macromolecules can be achieved without shear induced deformation or degradation. FlFFF has been widely used for the separation of biological particles such as bacterial ribosome subunits,[22,23] whole bacterial cells,[21,24,25] lipoproteins,[26−28] red blood cells,[29] mitochondria,[30] exosomes,[31] and other cell components. While FlFFF has been employed for isolation of mitochondria and exosomes,[30,31] these studies were based on the size fractionation of subcellular species already separated by centrifugation-based methods, followed by proteomic analysis of the collected fractions.

This study aimed to develop a high speed and soft sorting method using asymmetrical FlFFF (AF4) channel for the isolation of subcellular species from cell homogenates in which cell debris and heavy subcellular species were removed using gentle centrifugation. Fractionation of cell homogenates by AF4 was first optimized using the steric/hyperlayer mode, in which the separation of subcellular species in a decreasing order of hydrodynamic diameter can be achieved. The organelle fractions were collected for examination of morphology using scanning electron microscopy (SEM), organelles were confirmed by Western blot analysis using organelle-specific markers, and proteomic analysis of each fraction was performed using nanoflow liquid chromatography-electrospray ionization-tandem mass spectrometry (nLC-ESI-MS/MS), as depicted in Figure 1. Fractions containing early eluting species were collected and reinjected into the AF4 for a fine separation of nuclei, lysosomes, and microtubules using different run conditions. The present study demonstrates that AF4 can be utilized for the high speed and selective isolation of organelles in an aqueous buffer solution without disrupting the subcellular species. This protocol can be used as a complementary method for studying subcellular proteins and lipids for future biomarker development.

EXPERIMENTAL SECTION

Materials and Reagents. Protein standards and the following chemicals were purchased from Sigma-Aldrich (St. Louis, MO, U.S.A.): bovine serum albumin (BSA 66 kDa), thyroglobulin (670 kDa), NaCl, HEPES, $MgCl_2$, KCl, protease inhibitor cocktail, osmium tetroxide (OsO_4), Triton X-100, Tris-HCl, Trizma Base, sodium dodecyl sulfate (SDS), dithiothreitol (DTT), glycerol, bromophenol blue, Tween-20, ammonium persulfate, TEMED, glycine, urea, iodoacetamide (IAM), and cysteine. Polystyrene (PS) standards with nominal diameters of 1.999, 4.000, and 6.007 μm (hereafter referred to as 2, 4, and 6 μm) were from Thermo Fisher Scientific (Waltham, MA, U.S.A.). The blocking reagent used for Western blots and the protein quantification solution used in Bradford assays were obtained from Bio-Rad Laboratories, Inc. (Hercules, CA, U.S.A.). Primary antibodies including rabbit-α-LAMP2, rabbit-α-fibrillarin, mouse-α-ATPB (ATP synthase subunit beta), rabbit-α-tubulin, mouse-α-58K, rabbit-α-calnexin, and rabbit-α-catalase were purchased from Abcam Plc. (Cambridge, U.K.). Secondary antibodies including antirabbit-IgG (HRP-linked) and antimouse-IgG (HRP-linked) were purchased from Cell Signaling Technology, Inc. (Danvers, MA, U.S.A.). The protein ladder used in polyacrylamide gel electrophoresis was PageRuler from Pierce Biotechnology (Rockford, IL, U.S.A.). For chemiluminescence detection, the EZ-Western Lumi Femto solution from Daeil Lab Service Co. Ltd. (Seoul, Korea) was used. HPLC solvents (acetonitrile, methanol, and water) were from J.T. Baker, Inc. (Phillipsburg, NJ, U.S.A.). For proteolysis, proteomics grade trypsin from Promega Corp. (Madison, WI, U.S.A.) was used.

Cell Culture and Homogenization. The Human Embryonic Kidney 293T cell line (HEK 293T) was obtained from Severance Hospital (Seoul, Korea). Cells were grown in 100 mm culture flasks (72.3 cm^2) in Dulbecco's Modified Eagle's Medium (DMEM) from Invitrogen (Carlsbad, CA, U.S.A.) with 10% heat inactivated fetal bovine serum (FBS) and 1% penicillin streptomycin added, in a 37 °C incubator with 5% CO_2. When cells reached 90% confluency within 48−72 h, cells were detached by adding 0.25% trypsin-EDTA (Invitrogen) to allow for subculturing.

Cells (about 1×10^7 cells/mL) detached from the culture flask were centrifuged at 200g for 4 min to remove the trypsin-EDTA, mixed with 4 mL of 0.1 M PBS solution, and centrifuged for 4 min at 200g. The remaining cells were dispersed in 5 mL of a hypotonic lysis buffer solution[32] containing 10 mM HEPES, pH 7.9, 1.5 mM $MgCl_2$, 10 mM KCl, 0.5 mM DTT, and protease inhibitor cocktail and incubated at 4 °C for 5 min. The mixture was transferred to a 7 mL Dounce homogenizer (30 strokes with a tight pestle) from Wheaton (Millville, NJ, U.S.A.). The homogenate was centrifuged at 15000g for 10 min to remove heavy organelles and the supernatant solution (~4 mL) was collected for

DOI: 10.1021/acs.analchem.5b01207
Anal. Chem. 2015, 87, 6342−6348

organelle separation by FlFFF. The homogenate used in FlFFF is stored at 4 °C and only used within 24 h to prevent potential damage of organelles due to its low osmolality.

FlFFF. The FlFFF channel system used in this study the model LC (Long Channel, 275 mm length), an asymmetrical type of FlFFF (AF4) channel from Wyatt GmbH (Dernbach, Germany). The channel space was cut in a trapezoidal design: an inlet breadth of 2.2 cm decreased to 0.6 cm at the outlet, 26.6 cm long in a 250 μm thick Teflon sheet with a geometrical volume of 0.90 mL. For the channel membrane, a NADIR regenerated cellulose membrane sheet (MWCO 10 kDa) from Microdyn-Nadir GmbH (Wiesbaden, Germany) was utilized. For sample injection, a model 7125 injector (100 μL loop) from Rheodyne (Cotati, CA, U.S.A.) was placed before the sample inlet of the AF4 channel, as shown in Figure S1 in Supporting Information. Delivery of the carrier liquid to the AF4 channel was accomplished using a Model SP930D HPLC pump from Young-Lin Instrument (Seoul, Korea). Carrier solutions were prepared with deionized water containing 0.1% FL-70 from Thermo Fisher Scientific (Waltham, MA, U.S.A.) added with 0.02% NaN_3 for PS separation and 0.1 M PBS solution for the separation of cell homogenates. Separation of organelles was performed using the following procedures. The composition of FL-70 is in Supporting Information. Cell homogenate (100 μL) was loaded in the injector and delivered to the AF4 channel with a carrier liquid using the focusing/relaxation mode in which the 2.5 mL/min of carrier liquid was split to the inlet and outlet at a ratio of 1:9 using both 3-way and 4-way valves and all liquid exited through the channel wall, as shown in the dotted line configuration in Figure S1. Sample components were focused and accumulated at equilibrium at or around a position, 2.6 cm from the channel inlet, for 5 min. After focusing/relaxation, the flow direction was changed to the configuration depicted by the solid line so that the pump flow was delivered only to the channel inlet at an increased flow rate, $\dot{V}_{in}$ = 4.5 mL/min, and separation began. During the separation mode, the outflow rate ($\dot{V}_{out}$) was adjusted to 2.0 mL/min so that the crossflow rate ($\dot{V}_c$) was maintained at 2.5 mL/min. Monitoring of eluting subcellular species was performed with a model UV730D UV detector from Young-Lin at a wavelength of 280 nm and the detected signals were recorded using Autochro-Win 2.0 plus software from Young-Lin. Organelle fractions collected during FlFFF separation were used in secondary analyses with SEM, Western blot, and nLC-ESI-MS/MS.

SEM of Organelle Fractions. During the AF4 separation of cell homogenates, four fractions were collected at time intervals of 0.7−1.7, 1.7−3.7, 5.2−8.0, and 8.5−12.0 min. Five AF4 runs were performed to accumulate organelle fractions for SEM analysis. Each fraction was concentrated to about 1 mL by using an Amicon Ultra-15 centrifugal filter unit (10 kDa NMWL) from Millipore (Danvers, MA, U.S.A.) centrifuged at 2000g for 10 min at 4 °C. Each concentrated solution of the organelle fraction was slowly dropped on a (7 × 7 mm) polycarbonate membrane (pore size of 0.1 μm) from Millipore placed on a filter unit, the bottom part of which was connected with a syringe to pull the liquid in so that the dropped liquid was easily filtered through the membrane. After filtration, 100 μL of 2% OsO_4 solution was added to the filtrate on the membrane for fixation and an hour was allowed for the natural draining of the OsO_4 solution. After fixation, the OsO_4 fixed specimens were washed twice with 200 μL water and then dehydrated by flushing with a series of methanol solutions (30, 50, 70, and 100%). For each flush, 200 μL of each methanol solution was applied for 15 min and filtered by suction. After the dehydration steps, specimens on the membranes were dried and then sputtered with Pt for 120 s. SEM examination was performed at 5.0 kV of acceleration voltage using a JEOL-6701F Field Emission Scanning Electron Microscopy from JEOL Ltd. (Tokyo, Japan).

Western Blot Analysis of Organelle Fractions. For Western blot analysis of the organelle fractions collected from the AF4 runs, organelle proteins were released by adding Triton-X100 to each collected fraction followed by tip sonication (10 s pulse duration with 2 s intervals in 5 min).[30,31] Concentration of Triton-X 100 was kept at 0.1% (v/v) in order to filtrate organelle proteins efficiently in the purification step and to reduce interferences in UV absorbance measurement in Bradford assay. After lysis, the protein concentration of each fraction was measured using the Bradford method. From each fraction, 10 μg of protein was mixed with 5× Laemmli buffer solution (pH 6.8) containing 10% (w/v) SDS, 10 mM DTT, 50% (v/v) glycerol, 0.2 M Tris-HCl, and 0.05% (w/v) bromophenol blue and denatured at 90 °C for 5 min. The volume of the denaturation buffer solution used was 1/4 of the volume of the lysed protein solution. Gel electrophoresis of the denatured proteins was carried out on a 10% polyacrylamide gel using the Mini-PROTEAN Tetra Cell system from Bio-Rad Laboratories, Inc. (Hercules, CA, U.S.A.). The applied voltage used for protein migration was 80 V in the stacking gel and was increased to 150 V in the running gel. After electrophoresis, proteins were transferred to a nitrocellulose membrane (Bio-Rad) at 200 V for 1 h and the membrane was washed with 0.1 M TBS buffer with 0.1% Tween-20 for 5 min. Then, the membrane was blocked with a blocking solution (5% (w/v) skim milk in TBST) for 1 h and incubated with primary antibody at 4 °C overnight. After incubating with primary antibody, the membrane was washed with TBS for 30 min and incubated with secondary antibody (1/5000 (v/v)) at room temperature for 1 h. Chemiluminescence detection was performed with an LAS-4000 mini detector from GE Healthcare (Little Chalfont, U.K.).

nLC-ESI-MS/MS of Organelle Proteins. Each AF4 fraction was digested in-solution for proteomic analysis. Details of proteolysis can be found in Supporting Information. Protein analysis of the AF4 fractions was carried out with nLC-ESI-MS/MS: a model 1260 Capillary LC system equipped with an autosampler from Agilent Technologies (Waldbronn, Germany) and an LTQ Velos ion trap mass spectrometer from Thermo Finnigan (San Jose, CA, U.S.A.). For nLC separation prior to ESI, a trap column (2 cm × 200 μm i.d., 5 μm-200 Å Magic C18AQ from Michrom Bioresources Inc. (Auburn, CA, U.S.A.)) and an analytical column (7 cm × 75 μm i.d., 5 μm-100 Å Magic C18AQ) were connected via a PEEK microcross from IDEX (Oak Harbor, CA, U.S.A.), as shown in Figure S1. Columns were prepared in the laboratory using capillaries from Polymicro Technology, LLC (Phoenix, AZ, U.S.A.). Details of the packing procedure can be found in the literature.[33] Details of nLC-ESI-MS/MS can be found in Supporting Information.

RESULTS AND DISCUSSION

The separation of organelles by AF4 was evaluated using various flow rates and channel thicknesses. Figure 2 shows the fractograms of the HEK 293T cell homogenates obtained at different crossflow rates ($\dot{V}_c$), but using a fixed outflow rate, $\dot{V}_{out}$ = 2.0 mL/min, in 0.1 M PBS as a carrier solution. The

DOI: 10.1021/acs.analchem.5b01207
Anal. Chem. 2015, 87, 6342−6348

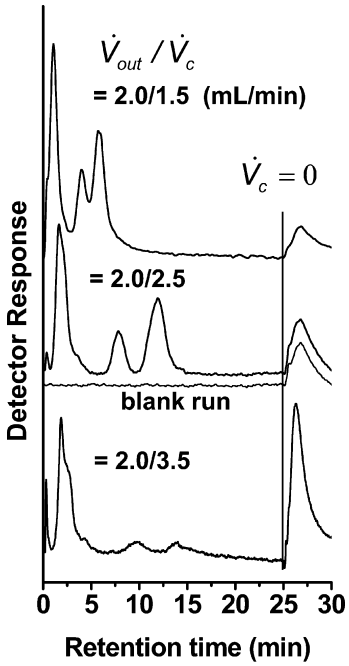

Figure 2. FlFFF fractograms of HEK 293T cell homogenate by varying crossflow rates ($\dot{V}_c$) from 1.5 mL/min to 3.5 mL min at a fixed outflow rate ($\dot{V}_{out}$), 2.0 mL/min in 0.1 M PBS solution. The crossflow rate was changed to 0 mL/min at 25 min.

fractogram of the cell homogenates at $\dot{V}_c$ = 1.5 mL/min (top) shows a substantial, large void peak, which is expected to contain some nonretained components such as large subcellular species or cytoplasmic proteins contained in homogenates, followed by two overlapping peaks. As the crossflow rate was raised to 2.5 and 3.5 mL/min, the intense peak at early retention times was divided into two peaks (a sharp void peak at the beginning and a large peak) presumably containing membrane debris or proteins. Separation of the two overlapping peaks found in the 3−10 min range of the top fractogram was improved and better resolution was obtained when the field strength, which refers to the strength of an external force generated by crossflow in FlFFF, was raised to $\dot{V}_c$ = 2.5 mL/min. However, the intensities of these two peaks were reduced significantly when $\dot{V}_c$ was further increased to 3.5 mL/min. In order to check for the presence of any remaining components in the channel, the field strength was set to zero at 25 min of elution. The small peaks that appear after 25 min in the top two fractograms were thought to be mostly from the system pulse due to the pressure change when crossflow rate was turned off; a finding that was confirmed by a blank run using the same run condition shown in the middle of Figure 2. This system pulse was increased significantly in the bottom fractogram which may originate from the larger pressure drop but it cannot exclude the possibility that a considerable amount of subcellular species could be dragged by the channel surface (membrane) under a strong field strength. While the channel thickness used for Figure 2 was 250 μm, we also tested channels of 190 and 150 μm since separation in steric/hyperlayer mode of FlFFF can be enhanced by reducing channel thickness, resulting in a decrease in zone broadening. However, separation was not improved much, and no additional elution of strongly retained components was seen. As the channel thickness was increased to 350 μm, the second and third peaks were not successfully resolved, as shown at the bottom of Figure S2a. Thus, the run condition using $\dot{V}_{out}/\dot{V}_c$ = 2.0/2.5 mL/min in a 250 μm thick channel was selected for subsequent separation of the cell homogenates.

Figure 3a shows the superimposed fractograms of cell homogenates from five repeated injections at $\dot{V}_{out}/\dot{V}_c$ = 2.0/2.5

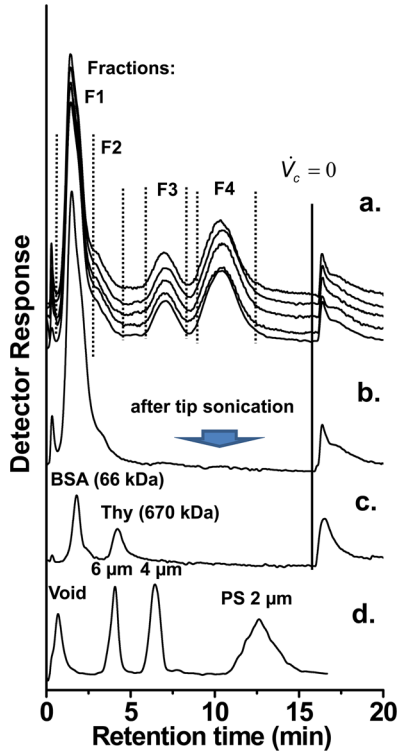

Figure 3. (a) Superimposed fractograms of HEK 293T cell homogenate obtained by five repeated FlFFF runs. Four fractions were collected at time intervals of 0.7−1.7, 1.7−3.7, 5.5−7.9, 9.0−12.0 min, respectively. (b) Fractogram of the cell homogenate sample after tip-sonication, (c) separation of BSA and thyroglobulin, and (d) separation of PS standard mixtures. The crossflow rate was turned off at 17 min in a−c. Carrier solutions were 0.1 M PBS for runs a−c and 0.1% FL-70 with 0.02% NaN_3 for run d. All runs were obtained at $\dot{V}_{out}/\dot{V}_c$ = 2.0/2.5 mL/min.

mL/min, showing good reproducibility of retention time and resolution together with consistent peak intensities of the transient peaks after turning off the field. Fractions of cell homogenates collected from AF4 separations were accumulated for 5, 10, and 10 repeated runs for SEM, Western blot, and proteomic analysis using nLC-ESI-MS/MS, respectively. For each run, 100 μL of homogenate sample was injected. Collection time interval for each fraction is listed in Table 1. In order to confirm that the eluted species in the F3 and F4

Table 1. Sizes of the Observed Subcellular Species in Each Fraction Measured from SEM Images

fraction # (shape)	time (min)	length (μm)	width (μm)	number counted
F1	0.7−1.7	6.23 ± 2.08	3.65 ± 0.91	10
F2	1.7−3.7	4.36 ± 1.09	1.60 ± 0.72	11
F3 (rods)	5.5−7.9	1.88 ± 0.46	0.45 ± 0.09	34
F4 (rods)	9.0−12.0	0.83 ± 0.14	0.59 ± 0.17	15
F4 (spheres)	9.0−12.0	0.67 ± 0.14[a]		21

[a]Diameter.

DOI: 10.1021/acs.analchem.5b01207
Anal. Chem. 2015, 87, 6342−6348

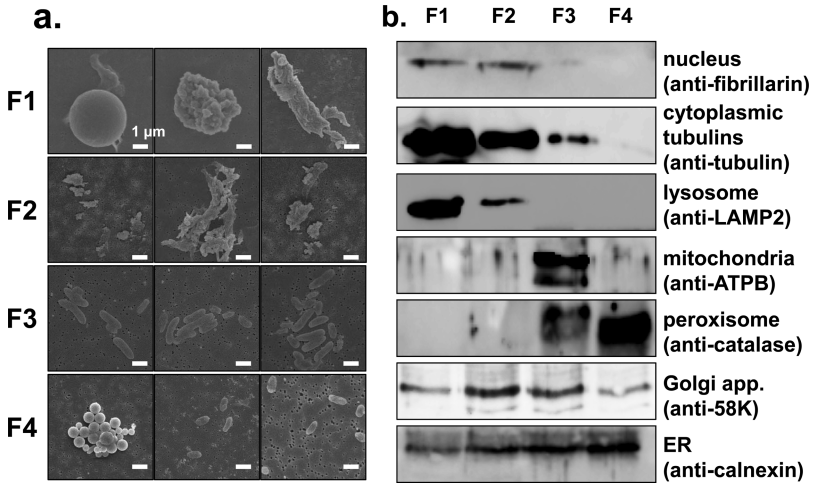

Figure 4. (a) SEM images of each fraction collected during FlFFF separation showing the different sizes and shapes of the observed particles. (b) Western blot analysis using organelle specific antibodies. Each lane was loaded with 10 μg of protein extract from each fraction.

fractions were subcellular components, the cell homogenate sample used for the AF4 separation was tip-sonicated for 5 min to disrupt organelles and the sonicated mixture was then injected to the AF4 channel at the same run condition used in Figure 3a. The resulting fractogram, shown in Figure 3b, demonstrates that the peaks observed in the 5−13 min range in Figure 3a disappeared with the increase in the peak intensity of the first peak, supporting the idea that the species in F3 and F4 were membrane-based subcellular particles. The possibility of elution of very high MW but free unbound proteins in the F3 and F4 peaks is relatively small, since MWs of most proteins in cells are less than a million. Based on the separation of protein standards (BSA, 66 kDa and thyroglobulin, 670 kDa) in the fractogram shown in Figure 3c, it can be estimated that the huge peak in Figure 3b fractogram may have originated from the increased amount of proteins (<100 kDa) caused by the disruption of organelles by sonication. The fractogram in Figure 3d represents a steric/hyperlayer separation of polystyrene (PS) standard latex particles (6, 4, and 2 μm in diameter) and provides an approximate size range of the species eluted in F3 and F4. PS separation was obtained using the same flow rate condition but using a different carrier solution (0.1% FL-70 plus 0.02% NaN_3 for particle separation).

After the calibration using PS particles, the channel membrane was replaced with a new one, and each of the four fractions (F1−F4) was collected from five repeated FlFFF runs and was examined by SEM, shown in Figure 4a. The SEM images of fractions F1 and F2 show relatively large species ($\gg$1 μm) with irregular shapes, except for a few spheres found in F1, which are likely agglomerations of cell wall debris, proteins possibly derived from ER, and a few submicrometer-sized subcellular species that were swept out without being resolved in the steric/hyperlayer separation conditions. While the first two fractions showed nonspecific shaped species, fractions F3 and F4 clearly contain organelles, with decreased sizes in the later fraction. The average diameter of particles measured in each fraction is listed in Table 1 and reveals that the average diameter or apparent length of particles decreased as retention time increased, thereby supporting the idea that these fractions were separated by the steric/hyperlayer elution mode of FFF. The contents of all fractions were further confirmed with Western blot by using seven organelle specific markers, especially focusing on membrane bound organelles (antitubulin for the presence of microtubules in the cytoplasm, antifibrillarin for nuclei, anti-LAMP2 for lysosomes, anti-ATPB for mitochondria, anticatalase for peroxisomes, anti-58K for Golgi apparatus, and anticalnexin for ER). The Western blot results from fractions F1 and F2, presented in Figure 4b, demonstrate the presence of tubulin (supporting the presence of cytoplasmic proteins) in both fractions. Lysosomes were enriched in F1, while nuclei (typically the largest organelle in cells) were found in both fractions. Since the homogenate sample was centrifuged at 15000g for 10 min during lysate preparation, most nuclei would be expected to have been removed. Therefore, the bands of the nuclei marker in Figure 4b are very dim compared to the bands of other markers. Moreover, antitubulin is a marker for tubulins in the cytoplasm[34] or microtubules that are long hollow cylinders made up of polymerized α/β-tubulin dimers thought to elute in the first peak due to their long dimensions. It is noteworthy that although lysosomes are known to be similar in size to mitochondria and peroxisomes,[2,35,36] the lysosomes in our experiment are clearly separated from the mitochondria and peroxisomes. We presumed that lysosomes appeared in this experiment were either much larger or even smaller than the other two organelles as they eluted at short retention times according to the steric/hyperlayer mode of separation. From the SEM image and a report that lysosomes may increase in size by aggregation,[37] they were thought to be aggregated in the first AF4 separation. This is supported from the additional experiments in Figure 5 and will be discussed later. In order to further examine these two fractions (F1 and F2), they were collected for reinjection into the AF4 channel using a different flow rate condition, as will be shown later. While the organelles seen in the micrographs of F3 are mostly rod shape and were confirmed to be mitochondria in Figure 4b, smaller oblong particles were found in F4 together with spherical particles which were presumed to be the peroxisomes identified by the Western blot results of the F4 fractions. Therefore, according to Western blot analysis, the major components of F3 and F4 are expected to be mitochondria and peroxisomes, respectively. While mitochondria and peroxisomes are known to be similar in size,[2] both were clearly separated in the AF4 experiment due to their differences in shape. Components of Golgi and ER were found in all fractions, as shown in Figure 4b, but they appeared to be more concentrated in F2 and F4, respectively. There is no clear

DOI: 10.1021/acs.analchem.5b01207
Anal. Chem. 2015, 87, 6342−6348

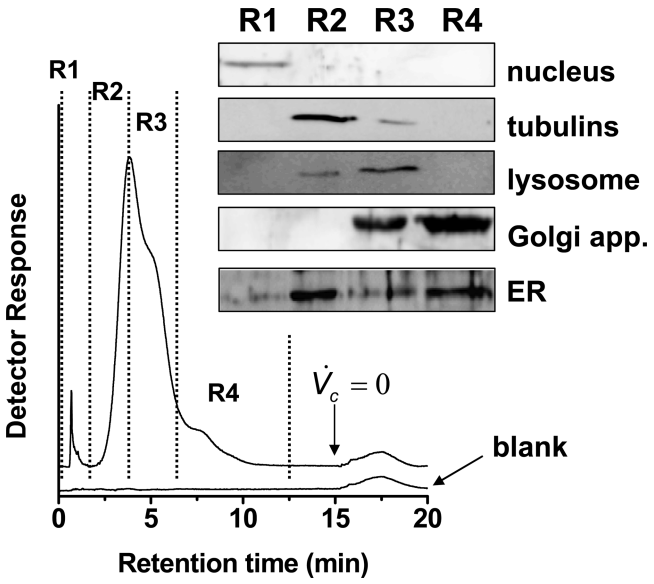

Figure 5. Fractogram of the combined fractions (F1 and F2) that were reinjected into the FlFFF channel to resolve organelles using the normal mode of separation and the corresponding Western blot results from the four fractions (R1−R4). Flow rate conditions were $\dot{V}_{out}/\dot{V}_c$ = 0.5/2.5 mL/min.

explanation as to why they appeared throughout the fractions. The Golgi apparatus and ER are known to be nonspecific in size and shape.[36] Instead, it is possible that these organelles were associated with other organelles, resulting in their coelution, or aggregation of proteins may result in the presence of ER throughout the fractions.

Confirmation of organelles was obtained by proteomic analysis of each fraction by using nLC-ESI-MS/MS and the number of identified proteins belonging to each subcellular location was grouped into two groups (F1 plus F2 vs F3 plus F4) in Table 2. The number of proteins that belong to the cytoplasm, nucleus, and lysosome (including endosome and exosome) identified by nLC-ESI-MS/MS as being exclusively present in fractions F1 + F2 is larger than those present in F3 + F4 (Table 2), while mitochondrial and peroxisomal proteins are exclusively enriched in fractions F3 + F4. The numbers listed

Table 2. Number of Proteins Belonging to Different Subcellular Locations Identified in Fractions F1 + F2, F3 + F4, and All Fractions[a]

subcellular location (multiple location)	F1 + F2 only	F3 + F4 only	both fractions	net
cytoplasm	172(52)	86(6)	98(12)	356(77)
nucleus	87(51)	3(4)	2(7)	92(62)
lysosome, endosome, exosome	12(10)	2(1)	0(2)	14(13)
mitochondrion	10(2)	57(4)	23(7)	90(13)
peroxisome	0(0)	12(2)	1(1)	13(3)
ER	16(5)	3(1)	15(1)	34(7)
golgi apparatus	9(3)	4(0)	11(2)	24(5)
others	71(3)	42(2)	23(2)	138(7)
total number of unique proteins	377(63)	209(11)	173(16)	759(90)

[a]A pair of numbers representing the protein numbers classified as being present in a single location, with the numbers in parentheses indicating proteins present in multiple locations.

for each organelle are represented in two ways; the number of unique proteins found only in either fraction is paired together with the number in parentheses which represents proteins counted in multiple locations. The data in Table 2 supported the expectations derived from the Western blot results of the collected fractions from the AF4 separation. Details of the proteins belonging to lysosomes, mitochondria, and peroxisomes are presented in Tables S1, S2, and S3 of Supporting Information, respectively. It is noted that lysosomal proteins and exsosomal proteins are found mostly from F1 and F1 + F2, respectively, in Table S1. Moreover, mitochondrial and peroxisomal proteins are enriched in F3 and F4, respectively, in Tables S2 and S3.

To achieve a better separation of the organelle species found in fractions F1 and F2, both fractions were collected from 10 additional runs and a mixture of the F1 and F2 fractions was reinjected into the AF4 channel using different run conditions of $\dot{V}_{out}/\dot{V}_c$ = 0.5/2.5 mL/min, which is a much lower outflow rate compared to that used in Figure 3 and similar to the run condition for normal mode of separation.[26] The small peak which appeared after the field-off at 15 min in Figure 5 was the system pulse which had a peak area nearly the same as that of a blank run. In addition, the eluent from the system pulse was collected for Bradford assay and used to confirm that neither proteins nor any organelles were present in the system pulse. The intense peak was clearly separated from a void peak (at ∼1 min) as the outflow rate was reduced in the reinjection run. Moreover, it appeared to be resolved better than the former separation condition in Figure 3, therefore the four fractions (R1, 0−2.0 min; R2, 2.0−4.5; R3, 4.5−7.0; and R4, 7.0−15 min) were collected and analyzed by Western blot. The inserted micrographs of Western blots in Figure 5 show that nuclei eluted with the void peak. This is because nuclei are much larger than other organelles, resulting in their being swept along with the void peak, rather than being retained, due to size effects in this run condition. Cytoplasmic proteins, including tubulins, were confirmed to be present in fraction R2 and clearly separated from nuclei. Moreover, lysosomes were found to be more concentrated in fraction R3 and Golgi apparatus, which was present in all fractions in the original run, were now more concentrated in R4. Since lysosomes are spherical and less than ∼1 μm in size, their separation in Figure 5 appears to be accomplished by the normal mode of FlFFF in which proteins of smaller sizes (less than 100 kDa typically) eluted earlier than larger ones. This may be explained as nonspherical particles, such as rods, which are usually less retained in FlFFF than spheres with diameter equivalent to the length of rods, due to the increase in the steric/entropic effect.[38,39] While fractions R2 and R3 were confirmed to contain tubulins and lysosomes, it cannot be excluded that the intense peak (R2 and R3) was largely contributed by the detection of cytoplasmic proteins.

CONCLUSION

This study provides a new guideline for the fast isolation/enrichment of subcellular organelles, without the use of a sucrose solution, allowing the collected fractions to be used in additional biological experiments for other purposes and it expands the potential utility of asymmetrical flow field-flow fractionation (AF4) for size sorting of subcellular organelles in cell homogenate mixtures. The present study demonstrated that a careful selection of the AF4 run conditions using a consecutive separation by reinjecting fractions collected from one run can be useful in the isolation/enrichment of target

DOI: 10.1021/acs.analchem.5b01207
Anal. Chem. 2015, 87, 6342−6348

organelles of interests. In addition, it was shown that the successful fractionation of organelles can be easily confirmed with SEM, Western blot, and proteomic analysis using nLC-ESI-MS/MS, without inducing any serious destruction of the organelles. While the recent centrifuge methods using sophisticated gradient media (iodinated or colloid-based) are known to provide efficient fractionation of organelles,[11,12] the separation of organelles by AF4 provides a speed in separation, a flexibility in handling cell homogenates with any biologically compatible buffer solution, and an advantage of fractionating organelles by size and shape factors, which are different from mass-based separation in centrifugation methods. While the current study demonstrates the potential to sort organelles by size, further optimizations are needed to improve the resolution of AF4 separations. It would be helpful to design experiments in such a way to increase throughput by constructing a preparative scale AF4 channel or employing a multiplexed hollow fiber FlFFF (MxHF5) so that sufficient amount of subcellular fractions can be retrieved.

■ ASSOCIATED CONTENT

Supporting Information

Additional information as noted in text. The Supporting Information is available free of charge on the ACS Publications website at DOI: 10.1021/acs.analchem.5b01207.

■ AUTHOR INFORMATION

Corresponding Author

*Phone: (82) 2 2123 5634 . Fax: (82) 2 364 7050. E-mail: mhmoon@yonsei.ac.kr.

Notes

The authors declare no competing financial interest.

■ ACKNOWLEDGMENTS

This study was supported by the Grant NRF-2015004677 from the National Research Foundation (NRF) of Korea.

■ REFERENCES

(1) Yates, J. R., 3rd; Gilchrist, A.; Howell, K. E.; Bergeron, J. J. *Nat. Rev. Mol. Cell Biol.* **2005**, *6*, 702−714.
(2) Satori, C. P.; Kostal, V.; Arriaga, E. A. *Anal. Chim. Acta* **2012**, *753*, 8−18.
(3) Huber, L. A.; Pfaller, K.; Vietor, I. *Circ. Res.* **2003**, *92*, 962−968.
(4) Reddy, P. H.; Beal, M. F. *Brain Res. Rev.* **2005**, *49*, 618−632.
(5) Chan, D. C. *Cell* **2006**, *125*, 1241−1252.
(6) Lin, M. T.; Beal, M. F. *Nature* **2006**, *443*, 787−795.
(7) Meikle, P. J.; Hopwood, J. J.; Clague, A. E.; Carey, W. F. *J. Am. Med. Assoc.* **1999**, *281*, 249−254.
(8) Gould, S. J.; Valle, D. *Trends Genet.* **2000**, *16*, 340−345.
(9) Özcan, U.; Cao, Q.; Yilmaz, E.; Lee, A. H.; Iwakoshi, N. N.; Özdelen, E.; Tuncman, G.; Görgun, C.; Glimcher, L. H.; Hotamisligil, G. S. *Science* **2004**, *306*, 457−461.
(10) Schmidt, H.; Gelhaus, C.; Lucius, R.; Nebendahl, M.; Leippe, M.; Janssen, O. *BMC Immunol.* **2009**, *10*, 41−52.
(11) Sims, N. R.; Anderson, M. F. *Nat. Protoc.* **2008**, *3*, 1228−1239.
(12) Segle, P. O.; Brinchmann, M. F. *Autophagy* **2010**, *6*, 542−547.
(13) Hornig-Do, H. T.; Günther, G.; Bust, M.; Lehnartz, P.; Bosio, A.; Wiesner, R. J. *Anal. Biochem.* **2009**, *389*, 1−5.
(14) Wang, Y.; Taylor, T. H.; Arriaga, E. A. *Anal. Bioanal. Chem.* **2012**, *402*, 41−49.
(15) Wilson, R. B.; Murpphy, R. F. *Methods Cell Biol.* **1989**, *31*, 293−317.
(16) Cossarizza, A.; Ceccarelli, D.; Masini, A. *Exp. Cell Res.* **1996**, *222*, 84−94.
(17) Gauthier, D. J.; Sobota, J. A.; Ferraro, F.; Mains, R. E.; Lazure, C. *Proteomics* **2008**, *8*, 3848−3861.
(18) Giddings, J. C. *Anal. Chem.* **1981**, *53*, 1170A−1175A.
(19) Wahlund, K.-G.; Litzén, A. *J. Chromatogr.* **1989**, *461*, 73−87.
(20) Giddings, J. C. *Science* **1993**, *260*, 1456−1465.
(21) Reschiglian, P.; Zattoni, A.; Roda, B.; Casolari, S.; Moon, M. H.; Lee, J.; Jung, J.; Rodmalm, K.; Cenacchi, G. *Anal. Chem.* **2002**, *74*, 4895−4904.
(22) Nilsson, M.; Birnbaum, S.; Wahlund, K.-G. *J. Biochem. Biophys. Methods* **1996**, *33*, 9−23.
(23) Nilsson, M.; Wahlund, K.-G.; Bulow, L. *Biotechnol. Technol.* **1998**, *12*, 477−480.
(24) Lee, H.; Williams, S. K.; Wahl, K. L.; Valentine, N. B. *Anal. Chem.* **2003**, *75*, 2746−2752.
(25) Reschiglian, P.; Zattoni, A.; Roda, B.; Cinque, L.; Melucci, D.; Min, B. R.; Moon, M. H. *J. Chromatogr. A* **2003**, *985*, 519−529.
(26) Park, I.; Paeng, K.-J.; Yoon, Y.; Song, J.-H.; Moon, M. H. *J. Chromatogr. B* **2002**, *780*, 415−422.
(27) Rambaldi, D. C.; Zattoni, A.; Casolari, S.; Reschiglian, P.; Roessner, D.; Johann, J. *Clin. Chem.* **2007**, *53*, 2026−2029.
(28) Lee, J. Y.; Choi, D.; Johan, C.; Moon, M. H. *J. Chromatogr. A* **2011**, *1218*, 4144−4148.
(29) Barman, B. N.; Ashwood, E. R.; Giddings, J. C. *Anal. Biochem.* **1993**, *212*, 35−42.
(30) Kang, D.; Oh, S.; Reschiglian, P.; Moon, M. H. *Analyst* **2008**, *133*, 505−515.
(31) Kang, D.; Oh, S.; Ahn, S.-M.; Lee, B.-H.; Moon, M. H. *J. Proteome Res.* **2008**, *7*, 3475−3480.
(32) Brunner, E.; Ahrens, C. H.; Mohanty, S.; Baetschmann, H. b.; Loevenich, S.; Potthast, F.; Deutsch, E. W.; Panse, C. b.; De Lichtenberg, U.; Rinner, O.; Lee, H.; Pedrioli, P. G. A.; Malmstrom, J.; Koehler, K.; Schrimpf, S.; Krijgsveld, J.; Kregenow, F.; Heck, A. J. R.; Hafen, E.; Schlapbach, R.; Aebersold, R. *Nat. Biotechnol.* **2007**, *25*, 576−583.
(33) Kang, D.; Moon, M. H. *Anal. Chem.* **2006**, *78*, 5789−5798.
(34) Kurita, M.; Kuwajima, T.; Nishimura, I.; Yoshikawa, K. *J. Neurosci.* **2006**, *26*, 12003−12013.
(35) Rockstroh, M.; Müller, S. A.; Jende, C.; Kerzhner, A.; von Bergen, M.; Tomm, J. M. *OMICS* **2011**, *1*, 135−143.
(36) Satori, C. P.; Henderson, M. M.; Krautkramer, E. A.; Kostal, V.; Distefano, M. M.; Arriaga, E. A. *Chem. Rev.* **2013**, *113*, 2733−2811.
(37) Wang, H.-J.; Zhang, D.; Tan, Y.-Z; Li, T. *Am. J. Physiol. Cell Physiol.* **2013**, *304*, C617−C626.
(38) Beckett, R.; Giddings, J. C. *J. Colloid Interface Sci.* **1997**, *186*, 53−59.
(39) Alfi, M.; Park, J. *J. Sep. Sci.* **2014**, *37*, 876−883.

DOI: 10.1021/acs.analchem.5b01207
Anal. Chem. 2015, 87, 6342−6348